Current Research (2017) Newfoundland and Labrador Department of Natural Resources
Geological Survey, Report 17-1, pages 219-238

THE MICHELIN DEPOSIT: AN EXAMPLE OF ALBITITE-HOSTED URANIUM MINERALIZATION WITHIN THE CENTRAL MINERAL BELT OF LABRADOR

G.W. Sparkes, G.R. Dunning[1] and A. Langille[1]
Mineral Deposits Section
[1]Department of Earth Sciences, Memorial University of Newfoundland, St. John's, NL, A1B 3X5

ABSTRACT

The Michelin deposit represents the type example of albitite-type uranium mineralization within the Central Mineral Belt (CMB) of Labrador. Here, uranium mineralization is hosted within ca. *1860 Ma felsic volcanic rocks of the Aillik Group. New geochronological data from a coarse-grained, highly quartz- and feldspar-phyric metarhyolite dyke, representing the main host to uranium mineralization at the Michelin deposit, has produced a U–Pb age of 1848.4 ± 2.7 Ma. This age highlights the presence of a previously unrecognized intrusive event associated with the deposit and provides a new maximum age for the development of uranium mineralization, which is now bracketed between 1851 and 1800 Ma. Dating of a distinct marker unit within the deposit, known as the complex dyke, has produced a U–Pb age of 1854.5 ± 3.0 Ma; the sample also contains three generations of titanite, highlighting the complex thermal history associated with metamorphic and deformational events in the area.*

Geochemical data, from samples in the vicinity of the Michelin deposit, have outlined areas of anomalous uranium enrichment as well as potassium depletion, in association with the sodium metasomatism, linked with the formation of the albitite-type uranium mineralization. In addition, discrete zones of brecciation inferred to be associated with the overall mineralizing system have been recognized.

INTRODUCTION

The Michelin deposit represents the single largest defined uranium resource within the Central Mineral Belt (CMB) of Labrador, containing a NI 43-101 compliant resource of approximately 103 million lbs of U_3O_8 (Hertel *et al.*, 2009). As such, understanding the nature and timing of the associated mineralizing system has been of keen interest and the deposit has been the focus of academic studies (*e.g.*, Minatidis, 1976; Evans, 1980; Hicks, 2015). The style of mineralization developed at Michelin has most recently been defined as an albitite-type deposit (*e.g.*, Sparkes and Kerr, 2008; Wilde, 2013; Hicks, 2015; Sparkes, 2017a), also known as sodium-metasomatite-related mineralization. Within the Michelin deposit, finely disseminated uranium mineralization occurs in association with extensive zones of albitic alteration resulting from sodium metasomatism of deformed volcanic and plutonic rocks of the Aillik Group.

Previous U–Pb geochronological studies in the area bracketed the age of the mineralization to between 1860–1800 Ma (Sparkes and Dunning, 2015). The latter age constraint is provided by a post-mineralization quartz-feldspar-porphyry dyke, which crosscuts uranium mineralization at the Jacques Lake deposit (Sparkes and Dunning, 2009). In addition, previous results have identified several post-mineralization metamorphic events, the youngest of which is Grenvillian (Sparkes and Dunning, 2015). New U–Pb geochronological data from the deposit provides evidence for a previously unrecognized intrusive event within the volcanic stratigraphy, and also provides a younger maximum age constraint for the development of uranium mineralization.

The subsurface distribution of the albitic alteration related to the formation of the Michelin deposit has been the focus of previous studies (*e.g.*, Evans, 1980; Hicks, 2015). However, limited work has been conducted at surface with respect to outlining the distribution of similar styles of alteration. Detailed geochemical sampling of volcanic and plutonic rocks outcropping in the area of the Michelin deposit provides insight into the surficial distribution of albitic alteration. Results from this study, although hampered by a lack of outcrop in some locations, provide the first quantitative information regarding the extent of the sodium metasomatism around the Michelin deposit, and identifies a northeasterly trending zone of metasomatism, which is oblique to the main mineralized trend. Further work is required to fully understand the overall distribution of the alteration and the subsequent effects of the post-mineral deformation in the region.

CHARACTERISTICS OF ALBITITE-TYPE URANIUM MINERALIZATION

Albitite-type uranium mineralization, also referred to as sodium-metasomatites, primarily occur within two distinct periods of Earth's history, namely between 1900–1700 Ma and between 1500–1400 Ma (Cuney and Kyser, 2008), and it is largely found within Proterozoic metamorphic terranes, particularly those dominated by 2000–1800 Ma rocks (Wilde, 2013). Alkali metasomatism associated with this style of mineralization is commonly accompanied by albite enrichment and quartz dissolution, which can form pre-ore alteration halos such as that observed around some Iron Oxide-Copper Gold (IOCG) deposits, or as a syn-mineralization process associated with deep structures (Cuney and Kyser, 2008). The development of alkali metasomatism within uranium-mineralized districts typically has a structural control, often forming within ductile or cataclasis zones developed in regional-scale structures that can be traced for several tens of kilometres (*cf.* Cuney and Kyser, 2008; Wilde, 2013; Wilde *et al.*, 2013). The alteration associated with such structural zones is commonly more spatially extensive than the area of the uranium mineralization, which generally only represents a small portion of the overall metasomatic alteration. These mineralized zones typically range from several metres to several tens of metres in width, and extend for hundreds of metres along strike and at depth (Polito *et al.*, 2009; Cuney *et al.*, 2012). Such deposits typically occur as low grade (<0.2% U_3O_8; Dahlkamp, 1993; Cuney and Kyser, 2008), large tonnage deposits.

In association with the uraniferous zones, alteration assemblages are formed through the multi-stage development of sodic, calcic-magnesian and potassic metasomatism (Cuney and Kyser, 2008). In addition, breccias commonly display a spatial association with the metasomatic alteration (*e.g.*, Valhalla, Wilde *et al.*, 2013; Southern Breccia, Montreuil *et al.*, 2015; Michurinske, Cuney *et al.*, 2012). Uranium minerals developed in association with the sodium metasomatism commonly include uraninite, coffinite, brannerite and uraniferous zircon, and occur as fine-grained disseminations within the alteration (Wilde, 2013; Wilde *et al.*, 2013; Polito *et al.*, 2009; Cuney *et al.*, 2012). A spatial association between uranium- and titanium-bearing phases is also noted (Cuney and Kyser, 2008; Wilde, 2013). Gangue minerals associated with this style of mineralization include albite, carbonates, sodic pyroxene and amphiboles as well as fine-grained disseminated hematite and hydrothermal apatite (Wilde, 2013). Zircon can be mobile in zones of sodium metasomatism, and the development of hydrothermal zircon, forming overgrowths on existing magmatic zircons or locally filling veinlets, is noted to occur in association with the alteration (Cuney and Kyser, 2008; Cuney *et al.*, 2012)

PREVIOUS WORK

The Michelin deposit was discovered by Brinex in 1968, through follow-up exploration of an airborne radiometric survey. Several phases of mineral exploration have been carried out on the deposit since that time, along with a number of academic studies (*e.g.*, Gandhi, 1970, 1976, 1978; Watson-White, 1976; Minatidis, 1976; Bailey, 1979; Evans, 1980; Gower *et al.*, 1982; Wilton and Wardle, 1987; Sparkes and Kerr, 2008; Hicks, 2015), and have resulted in different depositional models being proposed for the genesis of the uranium mineralization.

Gandhi (1976) noted the relative narrow widths and considerable strike length of the mineralized zones, which were strongly controlled by stratigraphy, but also locally crosscut lithological contacts at shallow angles. Furthermore, he noted that such zones could be outlined on the basis of regional structure. Gandhi (1978) proposed a synvolcanic, magmatic origin for the mineralizing fluid responsible for the sodium metasomatism and related uranium mineralization, which he inferred to predate the final stages of deformation in the region.

Watson-White (1976) focused on the volcanic origin of the rocks hosting the Michelin deposit in addition to the strong alkali (sodium) metasomatism associated with the development of the uranium mineralization. This alteration was attributed to a synvolcanic process, but he noted that similar alteration occurred in shear zones elsewhere, where it was accompanied by local uranium enrichment (Watson-White, 1976). Minatidis (1976) carried out a comparative trace-element study of several uranium prospects in the CMB, noting that mineralized samples from the Michelin deposit contained higher concentrations of Zr, Zn and Ba and lower concentrations of Sr, Rb, Cu, Ni and Cr, relative to unmineralized samples in the area. He interpreted the sodium metasomatism to represent possible fenitization associated with the intrusion of carbonatites in the region.

Bailey (1979) described two main styles of mineralization in the western portion of the Aillik Group: 1) mineralization associated with shearing and faulting, and 2) stratigraphically controlled mineralization within felsic volcanic and sedimentary rocks. He inferred that the structurally controlled style of mineralization represented the remobilization of uranium from the surrounding country rock during Grenvillian deformation. The stratiform style of mineralization, to which the Michelin deposit was assigned, was inferred to be indicative of volcanogenic hydrothermal processes, but it was noted that a metamorphic origin was also possible for the mineralization occurring within the deposit (Bailey, 1979).

Evans (1980) outlined three main zones of alteration associated with the deposit on the basis of geochemistry; namely the transition, outer and inner alteration zones. He concluded that the U–Zr-bearing mineralizing fluid was oxidizing and sodium-enriched, and that the alteration was predominantly developed in the coarse-grained, porphyritic felsic volcanic units, which he concluded, represented preferential zones of fluid migration within the volcanic stratigraphy. The uranium was inferred to have been leached from the surrounding volcanic host rocks by neutral to weakly alkaline, oxidizing groundwater. Gower *et al.* (1982) favoured an epigenetic–hydrothermal model for the formation of the deposit, which was inferred to be coeval with the formation of the volcanic rocks of the Aillik Group. These same rocks were also inferred to represent the most plausible source for the uranium mineralization. Wilton and Wardle (1987) noted that the REE patterns for mineralized rocks from the Michelin deposit displayed similar patterns to the unmineralized host rocks. They also noted differences in the REE patterns of uranium mineralization at Michelin relative to other occurrences in the Aillik Group, near the Makkovik area. The former was attributed to represent syn- to post-volcanic products of hydrothermal leaching of volcanic glass, while the latter was inferred to be influenced by the emplacement of posttectonic granites.

Sparkes and Kerr (2008) provided a preliminary classification of the major uranium occurrences throughout the CMB, and characterized the mineralization in the Michelin area as being broadly metamorphic and/or metasomatic. The mineralization was noted to display similarities to ‘albitites’ or ‘Na-metasomatites’, most commonly known from the Baltic Shield region and Russia. The inclusion of the Michelin deposit within this classification is also discussed by Wilde (2013), Hicks (2015) and Sparkes (2017a). Hicks (2015) conducted a detailed petrographic and geochemical study of the Michelin deposit, focusing on the development of the sodium metasomatism and the related uranium mineralization. Detailed scanning electron microscope-mineral liberation analyzer (SEM-MLA) imagining of mineralized samples identified the presence of secondary zircon growth in association with the development of uranium mineralization; however, it was noted that this growth was largely confined to the outer rims of existing zircon crystals within the host rock. Hicks (2015) concluded that the uranium contained within the Michelin deposit was likely sourced from the surrounding felsic volcanic rocks of the Aillik Group. He classified the Michelin deposit as a Na-metasomatic uranium deposit, interpreted to have formed within a regional shear zone during the *ca.* 1900–1700 Ma Makkovikian Orogeny.

REGIONAL GEOLOGY

The Michelin deposit is hosted in the Aillik Group, and is composed of an upper greenschist- to lower amphibolite-facies Paleoproterozoic metasedimentary and metavolcanic supracrustal sequence, which is intruded by both foliated and nonfoliated intrusions ranging in age from *ca.* 1800–1630 Ma (Gower *et al.*, 1982; Kerr, 1994; Kerr *et al.*, 1996; Hinchey, 2007; Hinchey and LaFlamme, 2009). The Aillik Group forms part of the larger Aillik domain of the Makkovik Province that was accreted to the Nain cratonic margin during the Makkovikian Orogeny (Kerr *et al.*, 1996, 1997; Culshaw *et al.*, 1998, 2000; Ketchum *et al.*, 2002; Hinchey, 2007; Hinchey and LaFlamme, 2009). The lower stratigraphic portion of the Aillik Group is dominated by metasedimentary rocks that were originally sandstone, siltstone, conglomerate, and tuffaceous sandstone. It also contains minor volcanic rocks including felsic tuff, rhyolite, volcanic breccia, and mafic volcanic rocks and related volcaniclastic rocks. The upper part of the stratigraphy of the Aillik Group is dominated by metavolcanic rocks and consists of felsic to intermediate tuff, flow-banded rhyolite, quartz-feldspar porphyry rhyolite and lesser volcaniclastic material. The tectonic setting for the formation of the Aillik Group is not clearly defined, but more recent work suggests a shallow-marine to subaerial environment within an arc/rifted-arc to back-arc type setting (Wardle and Bailey, 1981; Gower *et al.*, 1982; Kerr *et al.*, 1996; Culshaw *et al.*, 2000; Sinclair *et al.*, 2002; Ketchum *et al.*, 2002), between *ca.* 1883–1856 Ma (Schärer *et al.*, 1988; Hinchey and Rayner, 2008).

Rocks of the Aillik Group are variably deformed, where deformation is commonly observed as large-scale anticlines and synclines forming gently plunging folds, and locally developed steeply dipping shear zones accompanied by upper greenschist- to lower amphibolite-facies metamorphism (Clark, 1979; Gower *et al.*, 1982; Culshaw *et al.*, 2000; Ketchum *et al.*, 2002; Hinchey, 2007; Hinchey and LaFlamme, 2009). The development of the steeply dipping shear zones within the main portion of the Aillik Group is attributed to a regional D_3 event representing sinistral transpression associated with the westward thrusting of the Aillik Group (Culshaw *et al.*, 2000; Hinchey and LaFlamme, 2009), and is broadly bracketed between *ca.* 1860–1800 Ma (Ketchum *et al.*, 2002). Locally, uranium mineralization displays a close spatial association with these structures, such as the Big Island shear zone of Ketchum *et al.* (2002; Figure 1). In addition, existing age constraints for uranium mineralization within the Aillik Group (*e.g.*, Sparkes and Dunning, 2009, 2015; Wilton *et al.*, 2010) are broadly similar to the age bracket of the D_3 deformational event.

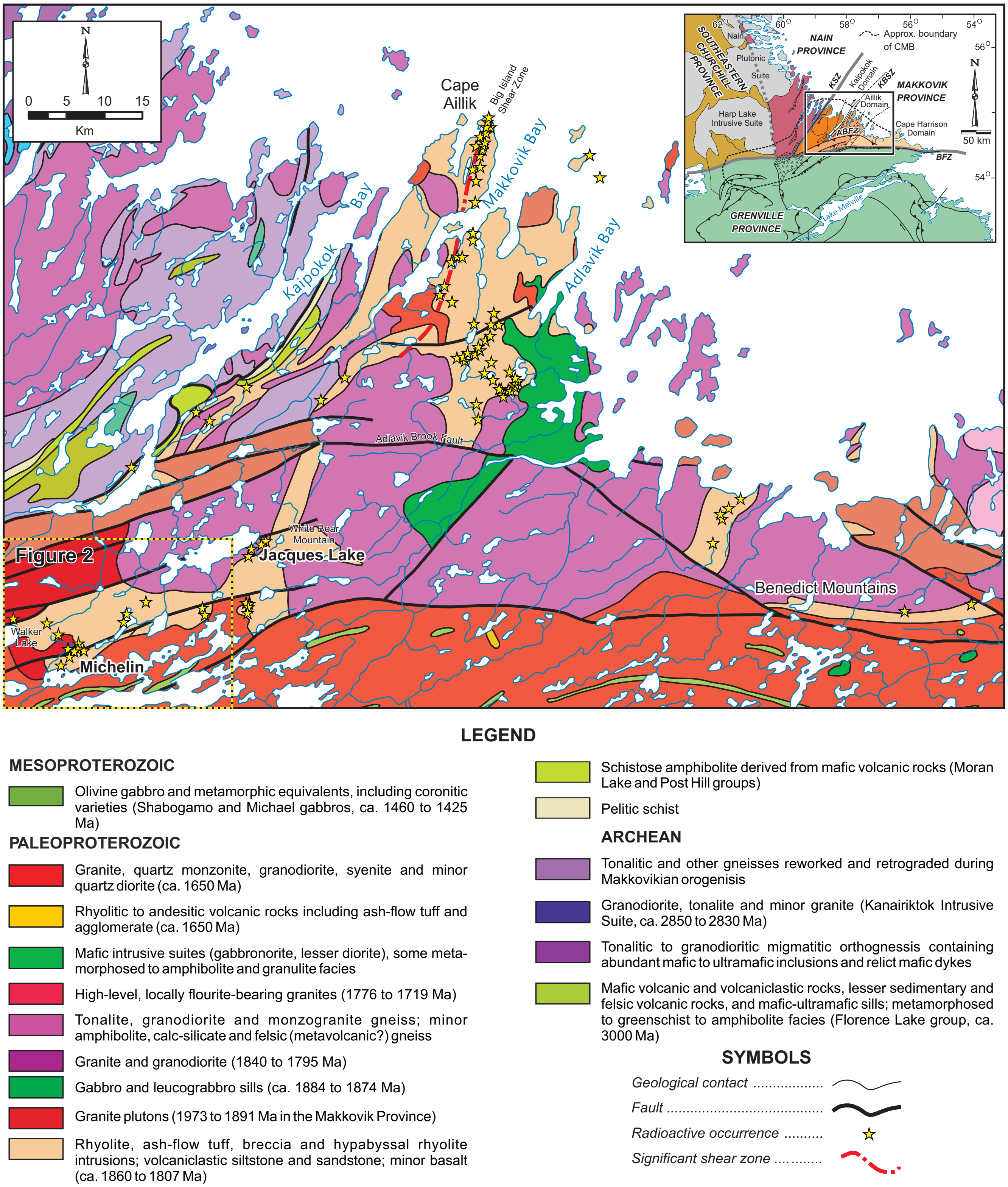

Figure 1. *Regional geology map outlining the distribution of known uranium occurrences hosted in Aillik Group rocks; geological base map modified from Wardle* et al. *(1997). Inset map outlines the regional subdivisions of the CMB; modified from Hinchey and LaFlamme (2009). BFZ – Benedict fault zone; KBSZ – Kaipokok Bay shear zone; KSZ – Kanairiktok shear zone; ABFZ – Adlavik Brook fault zone.*

GEOLOGY AND MINERALIZATION

LOCAL GEOLOGY OF THE MICHELIN DEPOSIT

The geology surrounding the Michelin deposit has been discussed in detail by Gandhi (1978, 1984), Bailey (1979), Evans (1980), Gower *et al.* (1982), Otto *et al.* (2013) and Hicks (2015). In general, the deposit is hosted by a mixture of variably porphyritic felsic volcanic and intrusive rocks, displaying varying intensities of deformation. These rocks contain mineral assemblages indicative of lower amphibolite-facies metamorphism, and are crosscut by both foliated and non-foliated intrusions (Figure 2). The succession forms a northeast-trending, southeast-dipping assemblage, inferred to young toward the south (Otto *et al.*, 2013). Due to the intense alteration associated with the development of uranium mineralization, combined with the effects of post-mineralization deformation, several different interpretations regarding the formational environment of the host rocks to the deposit have been proposed. Initial reports for the area interpreted the host rocks to be metasedimentary (Gandhi, 1969); however, subsequent work reinterpreted the sequence as subaerial ash-flow tuffs (Watson-White, 1976; Bailey, 1979; Evans, 1980; Gower *et al.*, 1982; Hicks, 2015)

In the immediate vicinity of the deposit, three main units host uranium mineralization and related alteration. The most abundant rock type within the volcanic stratigraphy consists of massive, crystal tuff containing moderately abundant, medium-grained, quartz and feldspar crystals (1–5 mm diameter) supported within a microcrystalline quartz-feldspar-rich matrix (sub-porphyritic metarhyolite unit of Evans (1980); fine-grained porphyritic metamorphosed felsic volcanic unit of Hicks (2015; Plate 1A). Coarse-grained, highly quartz- and feldspar-phyric metarhyolite dykes (coarse porphyritic metarhyolite unit of Evans (1980); coarse-grained porphyritic metamorphosed felsic volcanic unit of Hicks (2015); Plate 1B) occur as 2–30-m-thick sheets within the crystal tuff. This unit contains abundant phenocrysts (5–15 mm diameter) within a microcrystalline groundmass and is the main host to uranium mineralization (Figure 3). Contact relationships between the crystal tuff and the quartz- and feldspar-phyric metarhyolite dykes are variable, and have been described as both gradational (Evans, 1980; Hicks, 2015) and sharp (Otto *et al.*, 2013; Hicks, 2015) and are also locally defined by narrow shear zones or the intrusion of mafic dykes.

The nature of the quartz- and feldspar-phyric metarhyolite unit has been the focus of debate as to whether it represents a volcaniclastic deposit related to the deposition of the crystal tuff or a later subvolcanic intrusion. Gandhi (1978) referred to the entire sequence hosting the Michelin deposit as being variably porphyritic rhyolite, along with lesser tuffaceous material. Bailey (1979) interpreted the sequence as variably porphyritic, rhyolitic ash-flow tuffs. He noted that north of the main Michelin deposit, similar rocks displayed abundant primary volcanic features such as vitric fragments, lithic fragments, flow-banding, pyroclastic beds and welded textures, which provided supporting evidence for their subaerial origin. Evans (1980) also interpreted the sequence hosting the deposit as a sequence of subaerial ash-flow tuffs, based on their regional extent, uniformity, texture, composition and lack of bedding. Hicks (2015) noted the strong similarities between both the crystal tuff and the quartz- and feldspar-phyric metarhyolite (now recognized as an intrusive unit), which he inferred as supporting evidence for the formation of both units within a similar subaerial volcanic environment.

Hicks (2015) noted the presence of lithic fragments, which have been metamorphosed and deformed to biotite–hornblende-rich wisps, in both the crystal tuff and the quartz- and feldspar-phyric metarhyolite; however, such features are less abundant in the quartz- and feldspar-phyric metarhyolite. It was also noted that the deformed biotite–hornblende-rich wisps, could also potentially represent primary phenocrysts or a mixture of phenocrysts and lithic fragments. He discussed several scenarios and depositional settings for the units hosting the Michelin deposit that would account for the observed textural features, but favoured the scenario whereby the porphyritic and less porphyritic units, each represented individual eruptions related to different volcanic events. Interestingly, one of the scenarios proposed by Hicks (2015) indicated a plutonic origin for the quartz- and feldspar-phyric metarhyolite, occurring as syn-volcanic dykes or sills intruding the crystal tuff.

New geochronological data presented here for the quartz- and feldspar-phyric metarhyolite dykes (*see* below), indicate that the unit represents a porphyritic intrusion within the volcanic sequence, as demonstrated by the younger emplacement age of the dykes relative to that of the crystal tuff (Figure 4). However, the moderate to strong penetrative fabric developed within the vicinity of the deposit, combined with the effects of the alteration, often masks the original contact relationships within the mine sequence. Locally, as shown in Plate 1B, the contact between the quartz- and feldspar-phyric metarhyolite dykes and the adjacent crystal tuff is marked by the development of narrow, high-strain zones, illustrating the complex contact relationships developed within the deposit.

The origin of a second lithological unit, located within the hanging wall of the deposit, has also been a matter of debate. A mixed mafic–felsic porphyritic unit, measuring up to 10 m in width, crosscuts the crystal tuff and is commonly

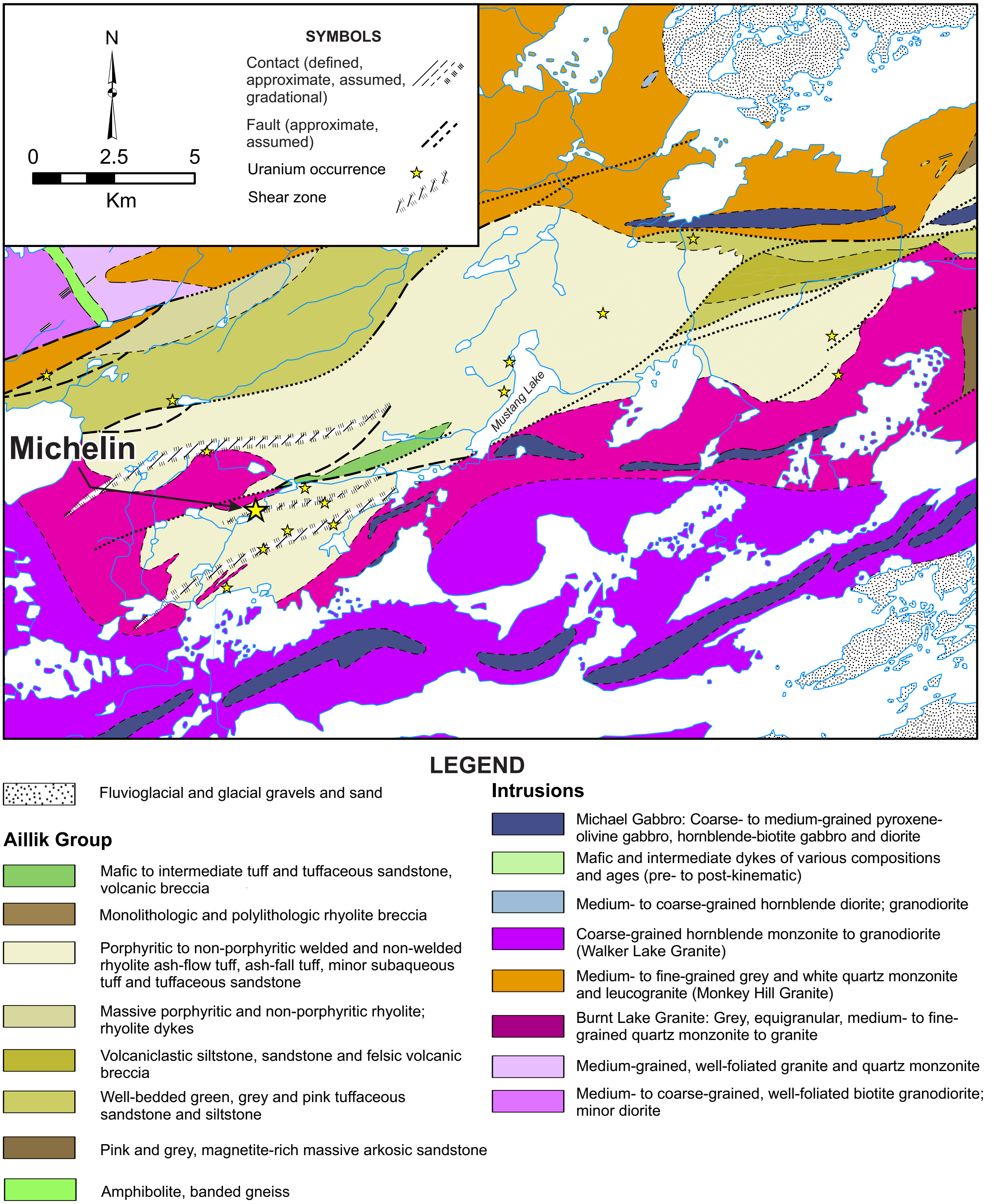

Figure 2. *Local geology map outlining the distribution of the main rock units and known uranium prospects in the area of the Michelin deposit; geological base map from Bailey (1979).*

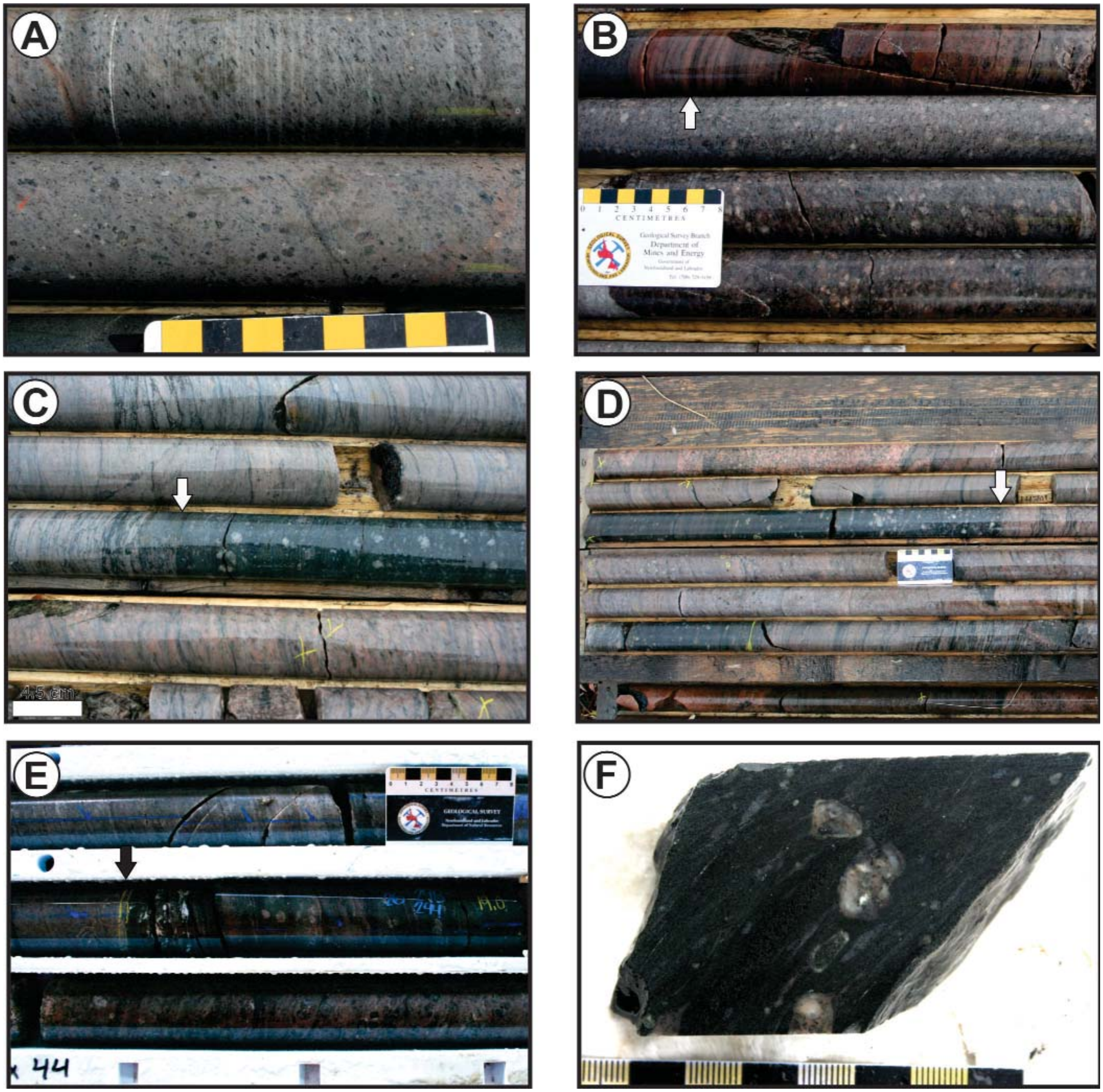

Plate 1. *A) Representative photograph of the massive, crystal tuff containing moderately abundant, medium-grained, quartz and feldspar crystals within a microcrystalline quartz–feldspar-rich matrix (DDH M06-13, 230 m); B) Coarse-grained, highly quartz- and feldspar-phyric, metarhyolite dyke; note the development of a 10- to 15-cm-wide mylonitic zone displaying hematitic alteration at the units upper contact with the crystal tuff (white arrow; DDH M06-11, 280 m); C) Sharp contact (white arrow) between the crystal tuff and the marginal, mafic-rich portion, of the complex dyke (DDH M08-114, 101.5 m); D) Photograph illustrating the relatively sharp transition into the coarse-grained, quartz- and feldspar-phyric felsic core of the complex dyke (white arrow; DDH M08-115, 148 m). Note the increased abundance of quartz and feldspar phenocrysts within the mafic portion of the dyke with decreasing distance from the contact with the felsic-rich core of the dyke; E) Complex dyke showing sharp contact (black arrow) between the crystal tuff (top) and the porphyritic, mafic-rich margin of the complex dyke (middle), which transitions to the more felsic-dominated porphyry core (bottom; DDH ML-163, 203 m); F) Representative sample of the porphyritic, mafic-rich margin of the complex dyke containing zoned feldspar phenocrysts within a fine-grained amphibolite groundmass (DDH ML-14-157, 70.5 m).*

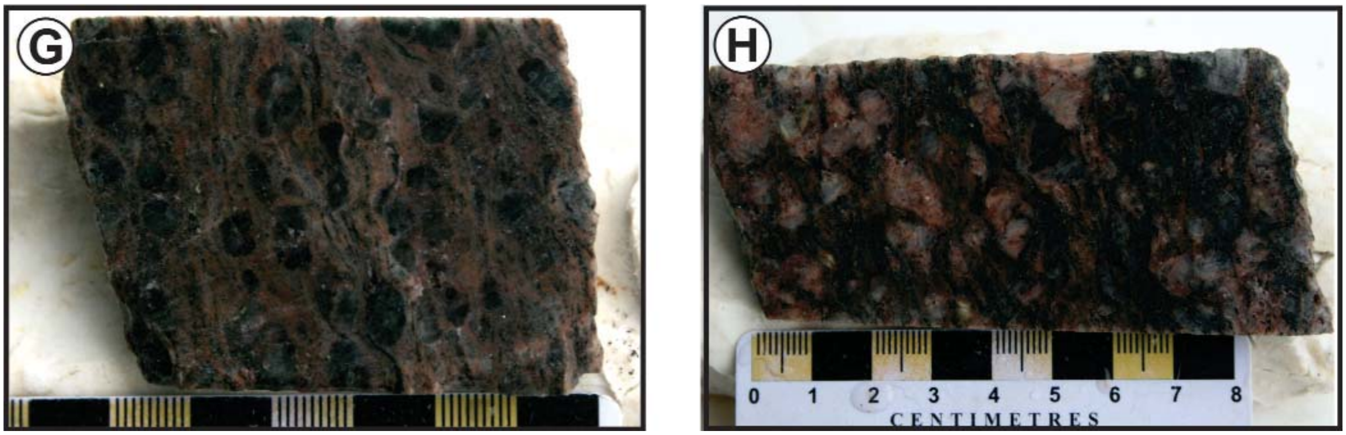

Plate 1. *(Continued) G) Variably developed coarse-grained, quartz- and feldspar-phyric core of the complex dyke (DDH ML-163, 203.7 m); H) Feldspar-rich portion of the felsic core of the complex dyke (DDH ML-163, 204.7 m).*

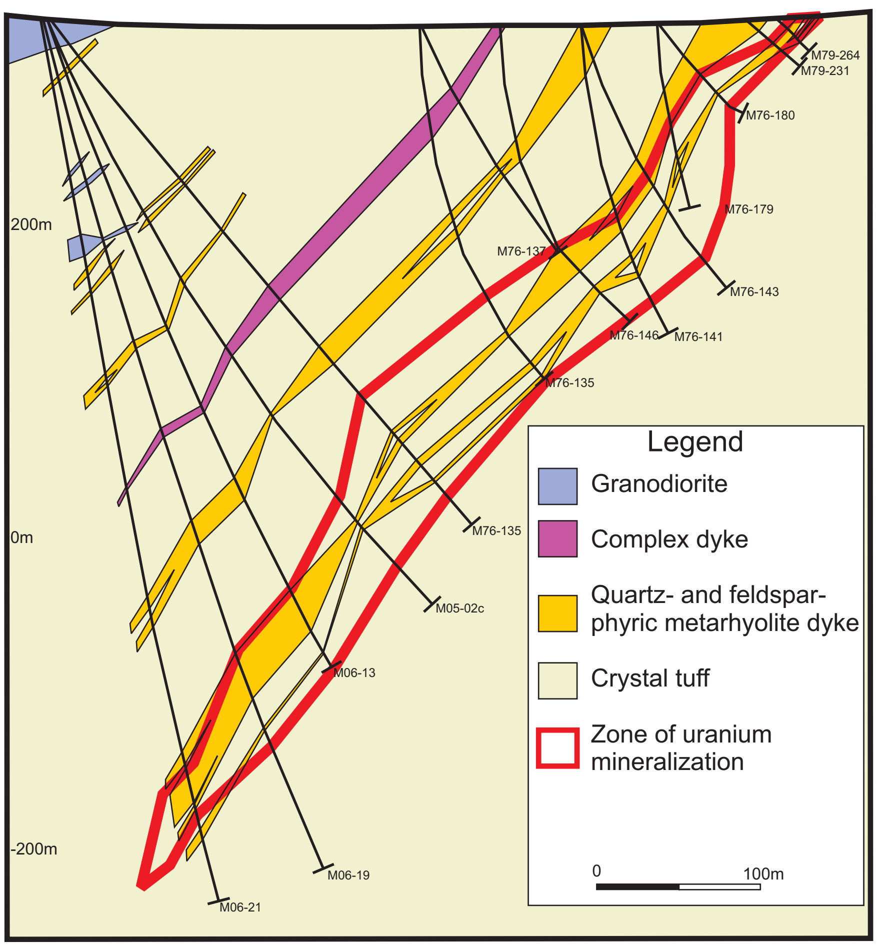

Figure 3. *Schematic cross-section through the Michelin deposit outlining the distribution of the main rock units and uranium mineralization; modified from Cunningham-Dunlop and Lee (2008). Note measurements on the left of the section denote metres above sea level.*

referred to as the 'complex dyke' (Piloski, 1976; Bailey, 1979; Sharpley, 1980). Piloski (1976) interpreted the unit to represent an intrusion, whereas Evans (1980) considered it to be volcanogenic. Sharpley (1980) interpreted the unit to represent a breccia zone infilled with fine-grained amphibolite containing fragments of partially recrystallized feldspar phenocrysts, but did not comment on the nature of its formation; however, he did note that the unit crosscut stratigraphy at a very shallow angle. This unit is locally overprinted by alteration related to the development of the albitite-hosted uranium mineralization.

The complex dyke represents one of the few distinctive marker units within the deposit, and is traced along its entire length, occurring at a predictable distance (between 55 to 67 m) above the main mineralized zone (Sharpley, 1980). The margins of the unit are commonly marked by a fine-grained amphibolite groundmass, which grades inward to a porphyritic amphibolite containing centimetre-scale feldspar and quartz phenocrysts (Plate 1C–F) and then to a quartz-feldspar porphyry core that forms the bulk of the unit (Plate 1G, H). The felsic-rich porphyry core displays similar features to the quartz- and feldspar-phyric metarhyolite dykes.

In the area of the Michelin deposit, a variably developed penetrative fabric, trending approximately 60° and dipping between 50–55° to the southeast, broadly parallels regional-scale shear zones defined by Bailey (1979; Figure 2). Within the deposit, a prominent lineation is developed that plunges 65° to the southwest and is parallel to the main mineralized zone (Gandhi, 1978). Bailey (1979) attributed the development of this schistose zone to an anticlinal axial zone related to tight isoclinal folding in the region. Although the mineralization and related alteration is inferred to be associated with the Makkovikian Orogeny (Wilton *et al.*, 2010; Hicks, 2015), geochronological evidence from the area also suggests the presence of a younger Grenvillian overprint (*cf.* Sparkes and Dunning, 2015).

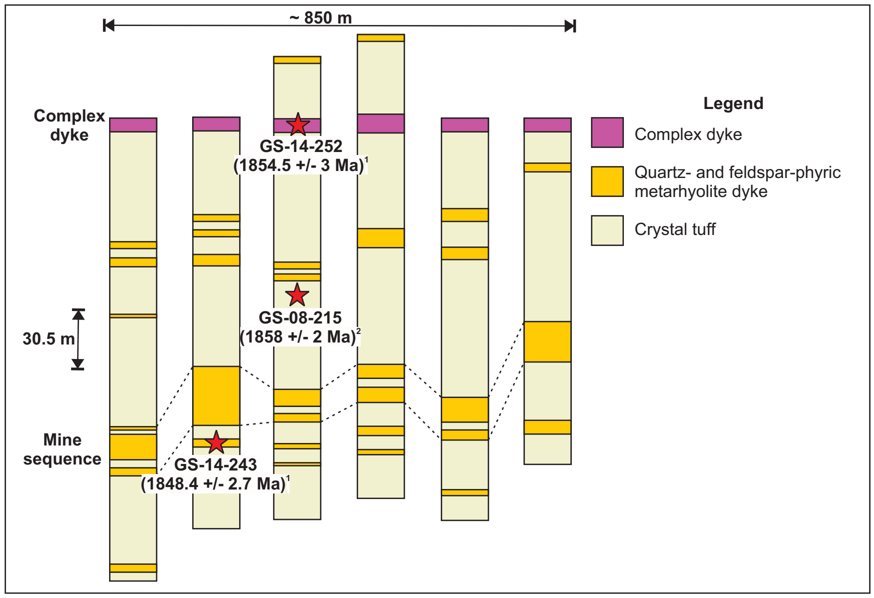

Figure 4. *Schematic, longitudinal section of the Michelin deposit outlining the distribution of the main rock units relative to the complex dyke as well as the approximate location of the geochronological samples collected from the area with their corresponding age determinations; modified from Sharpley (1980). Note the number following the age denotes the data source: 1)* this study*; 2) Sparkes and Dunning (2015).*

The volcanic sequence at the Michelin deposit is also crosscut by foliated and non-foliated intrusions and mafic dykes. The mafic dykes, some of which are weakly mineralized where they occur within the main mineralized zone (Gandhi, 1978), have variable relationships to the fabric, suggesting pre-, syn- and post-kinematic development. Hicks (2015) defined four main groups of dykes within the deposit, which are differentiated on the basis of deformation, texture and mineralogy. The earliest dykes, represented by the pre-kinematic dykes, are composed of biotite–hornblende schist. A second group, composed of gabbroic dykes, display moderate deformation and are inferred to have a syn-kinematic to late syn-kinematic timing of emplacement. Strongly magnetic gabbroic dykes and andesitic dykes, representing the third and fourth groups, respectively, both display little to no deformation, are inferred to be post-kinematic, and represent some of the youngest intrusions in the area. Granitoid plutonic rocks and quartz-feldspar porphyries forming subconcordant sheets within the metavolcanic host rock are inferred to postdate mineralization; such units have locally been dated at *ca.* 1640 Ma (Sparkes and Dunning, 2015).

SURFACE ALTERATION AND RELATED MINERALIZATION

The sodic-rich nature of the alteration associated with the development of uranium mineralization at the Michelin deposit has been well documented (Watson-White, 1976; Gandhi, 1978; Evans, 1980; Hicks, 2015; Sparkes, 2017a). Geochemical studies conducted by Hicks (2015) noted that unaltered crystal tuff in the area of the Michelin deposit contains an average of 3.7 wt. % Na_2O and 5.0 wt. % K_2O, while the quartz- and feldspar-phyric metarhyolite dykes contain 3.5 wt. % Na_2O and 5.6 wt. % K_2O. From a comparison of altered and unaltered units (on the basis of geochemical data and drillcore observations), he noted that samples containing >5.0 wt. % Na_2O displayed effects of sodium metasomatism. He also noted that the transition from unaltered to altered units occurred abruptly, generally within 10 m of the main alteration zone, and returned values of up to 10.1 wt. % Na_2O along with decreased values of K_2O. As is characteristic of this style of deposit, uranium mineralization postdates the sodium metasomatism and has a more restricted distribution (*cf.* Cuney and Kyser, 2008).

To illustrate the distribution of the albitic alteration exposed at surface in the vicinity of the Michelin deposit, outcropping units were sampled for geochemical analysis. As part of this study, 54 samples were collected, representing a combination of the crystal tuff and the quartz- and feldspar-phyric metarhyolite dykes within an area spanning some 6 x 5 km around the Michelin deposit. A map outlining the sample sites along with corresponding select geochemical values is shown in Figure 5A–C (data from Sparkes, 2017b). From the data, it is evident that not all samples in the immediate vicinity of the Michelin deposit display evidence of sodium metasomatism (Figure 5A). One

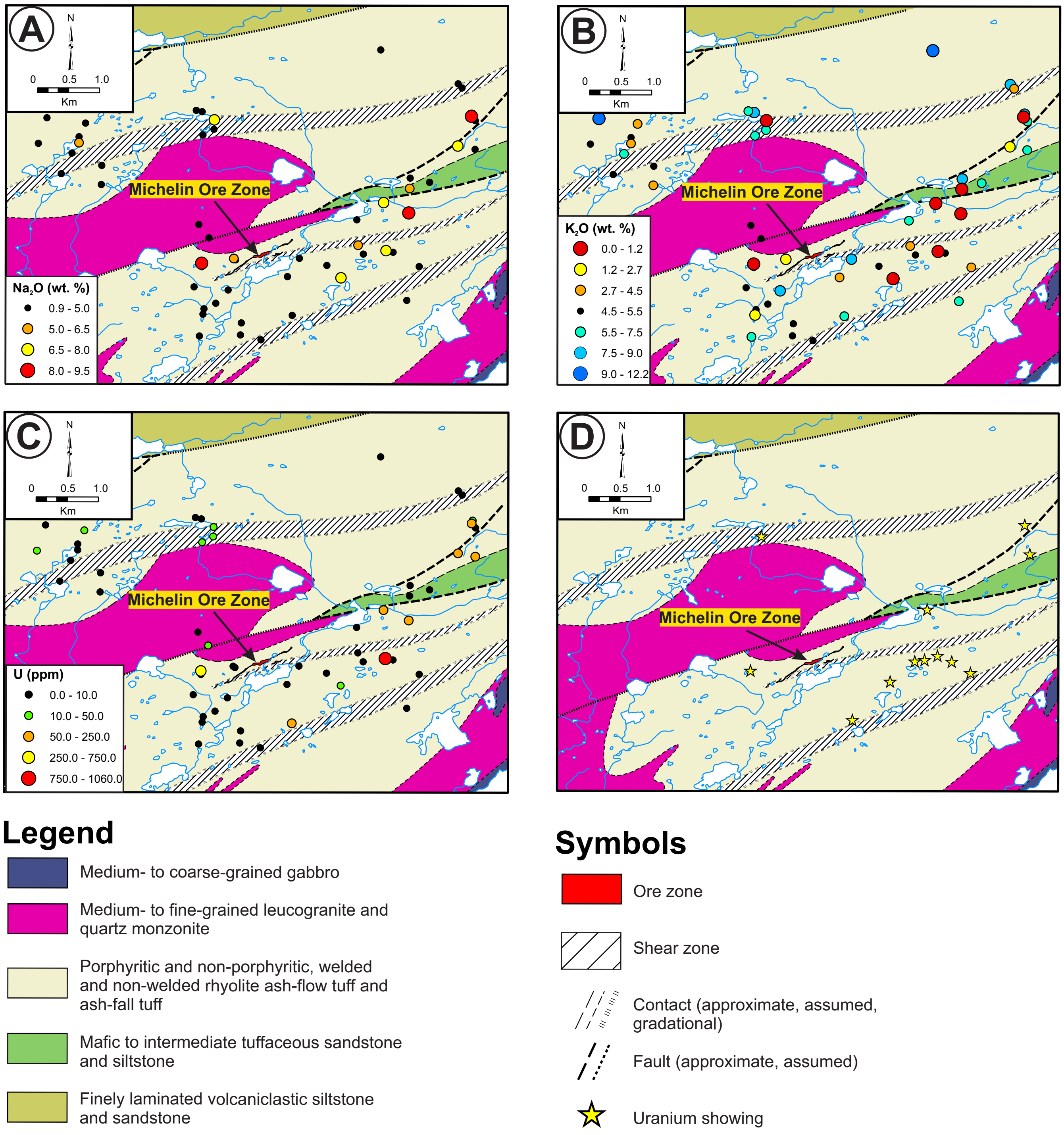

Figure 5. *Geochemical sample sites within the vicinity of the Michelin deposit displaying select results that outline the distribution of alteration associated with the formation of albitite-type mineralization in the area. Note, the surface projection of the Michelin ore zone as determined through exploration drilling is included for reference. A) Samples displaying Na_2O enrichment (>5.0 wt. %); B) Samples displaying K_2O depletion (<4.5 wt. %) in addition to local enrichment, indicating zones of possible potassic-style alteration; C) Samples displaying uranium enrichment (>10 ppm); D) Location of known uranium prospects in the vicinity of the Michelin deposit.*

particular feature observed from samples displaying sodium-enrichment is the apparent northeast–southwest trend of altered samples located to the east of the Michelin deposit (Figure 5A). This trend is oblique to the main mineralized zone at Michelin, as well as the predominant penetrative fabric developed within the host rocks in the area.

In addition to displaying sodium enrichment, samples occurring along this northeasterly trend also display significant depletion of potassium (Figure 5B) and local enrichment in uranium (Figure 5C). This northeasterly trending alteration zone also displays a spatial association with identified uranium prospects in the area (Figure 5D). The significant aerial extent of the sodium metasomatism developed in the area is highlighted by the occurrence of altered samples up to 3.6 km from the Michelin deposit.

STRUCTURE

The formation of albitite-type deposits characteristically displays an overriding structural control on the development of the metasomatic alteration and accompanying uranium mineralization. The structures commonly hosting the mineralizing systems are generally represented by regional-scale faults that can be traced for several tens of kilometres along strike (*cf.* Cuney and Kyser, 2008; Wilde, 2013; Wilde *et al.*, 2013). Regional mapping within the vicinity of the Michelin deposit has only identified discrete, relatively narrow, discontinuous shear zones, as opposed to a regionally significant structure. However, more detailed, property-level mapping conducted by exploration geologists has indicated the presence of thrusting within the Michelin deposit (Otto *et al.*, 2013), but as the mineralization is typically confined to areas of low topographic relief, outcrop in the area is poorly exposed, thereby making regional correlations difficult.

Despite the lack of a recognized regional structure within the immediate vicinity of the Michelin deposit, features observed within, and around, the area are indicative of a structural setting for the albitite-hosted mineralization. Brecciation is a common feature developed in association with the formation of albitite-type uranium mineralization (*e.g.*, Cuney *et al.*, 2012; Wilde *et al.*, 2013), but such textures have been poorly documented in the Michelin area. Field mapping conducted during the collection of geochemical samples identified several occurrences of brecciation in the area of the Michelin deposit. One such occurrence, developed in an area of relatively low strain, is composed of a jigsaw breccia having pale-pink angular fragments of crystal tuff hosted within a dark-green, amphibole- and magnetite-bearing matrix (Plate 2A, B). This breccia, however, was not associated with any sodic alteration or accompanying uranium mineralization.

Elsewhere in the region, in zones of relatively higher strain, magnetite-rich, cm-scale, zones of brecciation were locally identified (Plate 2C, D). The breccia veins trend perpendicular to the main east–northeast-trending foliation that overprints the brittle deformation. No associated sodium metasomatism or uranium enrichment accompanies this breccia development. Recognition of breccia textures is more challenging in drillcore given the limited surface area of the core, combined with the effects of the overprinting deformation. In rare instances, similar styles of brecciation to that observed in outcrop have been noted in core, and locally occur close to anomalous radioactivity (Plate 2E, F); however, no mineralized breccias have yet been identified in the area.

Drillcore from the deposit commonly contains a moderate to strong penetrative fabric, along with localized, narrow, mylonitic zones (Plate 3A). Within the deposit, the lack of distinct marker units hinder the evaluation of the degree of deformation developed within the host rocks, however, features observed at surface indicate that folding is locally developed (Plate 3B).

U–Pb GEOCHRONOLOGY

Two samples were collected from drillcore for geochronological study to further constrain the age of mineralization at the Michelin deposit. Samples were processed by standard techniques of crushing and concentration as previously described (*cf.* Sparkes and Dunning, 2014) resulting in heavy mineral separates of zircon and titanite. Zircon was chemically abraded following the procedure of Mattinson (2005), with annealing at 1000°C for 36 hours, followed by etching in concentrated hydrofluoric acid at 200°C for 4 hours. Lead and U isotopic ratios were measured by thermal ionization mass spectrometry and results calculated using ISOPLOT, for weighted averages, or by the technique of Davis (1982) for linear regression. Uncertainties on all ages are reported at the 95% confidence interval.

Previously reported ages for the volcanic rocks of the Aillik Group from within the vicinity of the Michelin deposit are 1856 ± 2 Ma (Schärer *et al.*, 1988) and 1858 ± 2 Ma (Sparkes and Dunning, 2015). The latter age targeted the unaltered equivalent of the crystal tuff (sub-porphyritic metarhyolite unit of Evans (1980); fine-grained porphyritic metamorphosed felsic volcanic unit of Hicks (2015)).

Due to the lack of distinct lithologies within the deposit, the complex dyke, one of the few uniquely distinguishable units traceable throughout the deposit, was sampled for geochronological study (Sample GS-14-252; DDH ML14-157, 73 m depth). The sample was collected from the

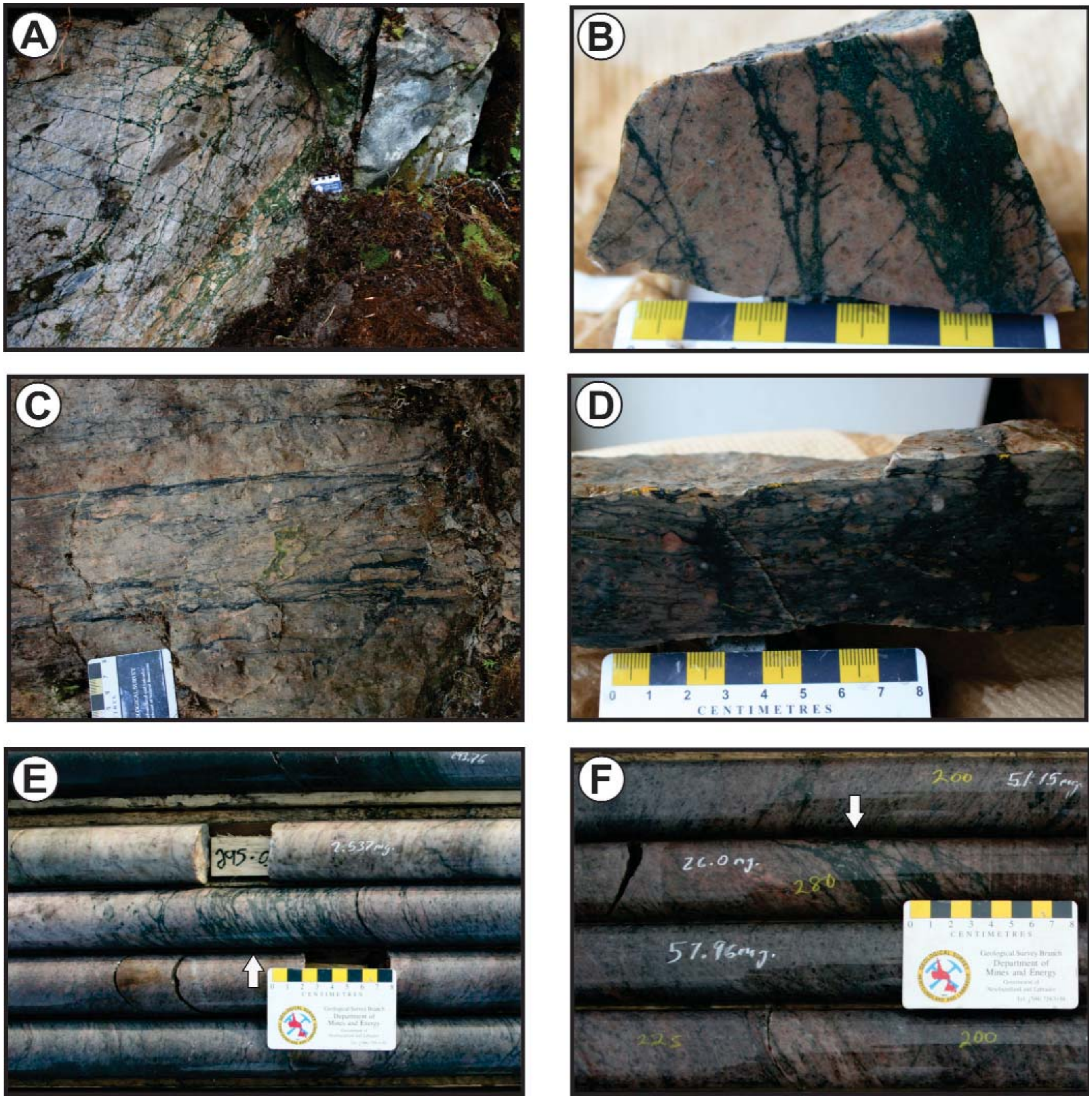

Plate 2. *A) Jigsaw-textured breccia containing an amphibole–magnetite-bearing matrix developed within crystal tuff approximately 0.5 km south of the Michelin deposit; note main breccia vein trends 60°; B) Cut sample of jigsaw breccia shown in (A); C) Centimetre-scale, magnetite-bearing, breccia veins developed within coarsely porphyritic metarhyolite occurring approximately 2.5 km northeast of the Michelin deposit; note breccia vein is perpendicular to the main penetrative fabric developed within the host rock, which trends approximately 75°; D) Cut sample of magnetite-bearing breccia vein shown in (C); E) Locally developed amphibole-rich breccia within relatively unaltered crystal tuff; DDH M07-072, ~295 m depth; F) Amphibole-rich brecciation developed marginal to mineralized zone; DDH M07-072, ~530 m depth.*

Plate 3. *A) Locally developed mylonitic texture within the crystal tuff unit, crosscut by a post-kinematic mafic dyke; DDH M07-075, ~ 380 m depth; B) Folded mafic dyke crosscutting the quartz- and feldspar-phyric metarhyolite dyke within the main exploration trench of the Michelin deposit.*

coarse-grained porphyritic felsic core of the dyke and displayed well-developed cm-scale subhedral phenocrysts of feldspar and finer grained quartz within a fine-grained groundmass of similar composition (Plate 4A). This sample yielded a large amount of coarse euhedral zircon, which displays internal complexities illustrated by the corrosion of growth zones, and development of new growth zones (Plate 4B); it also contains titanite of different colours, ranging from clear, colourless to dark brown. In addition, there were some titanite grains with obvious overgrowths of one colour of titanite on corroded cores of a different appearance.

Four analyses were carried out on fractions composed of 1 to 5 crystals of zircon, producing results that are concordant to 1.3% discordant with $^{207}Pb/^{206}Pb$ ages ranging from 1852 ± 8 to 1857 ± 7 Ma (Table 1, Figure 6A). These yield a weighted average $^{207}Pb/^{206}Pb$ age of 1854.5 ± 3 Ma (MSWD = 0.36), which is interpreted to be the igneous crystallization age of this unit. Eight analyses were carried out on titanite of different colours (6 single-grain fractions and two fractions consisting of 2 or 3 similar grains). The four analyses of clear grains (T1–T4, Table 1) contrast with those of dark brown (T5–T8, Table 1) mainly in the higher uranium content of the brown grains. As well, the four high-uranium dark-brown grains all represent one metamorphic generation, but the clear grains have different histories and both older and younger ages compared to the population of brown grains. Analyses of the dark-brown grains; T5, T6, T7 and T8 cluster around 1630 Ma on concordia (Figure 6A), with T8 slightly to the left of the concordia curve as a result of a shift due to its common lead content. The $^{206}Pb/^{238}U$ ages of these 4 analyses range from 1623 ± 16 (T8) to 1651 ± 35 Ma (T6). A weighted average $^{206}Pb/^{238}U$ age of the three best analyses (T5, T6, T7) yields 1638 ± 7.5 Ma (MSWD=0.35). If T8 is included this drops to 1635 ± 7 Ma.

Two analyses of single, clear titanite grains (T1, T4, Figure 6A) plot younger than the cluster at 1638 Ma, and a line calculated through these two analyses and T5, T6 and T7 yields an upper intercept at 1634 ± 40 Ma and a lower intercept of 1057 ± 140 Ma (88% probability of fit). T1 is only 3.8% down the line from 1638 Ma, while T4 is 43% discordant on this line. Two analyses, consisting of 1 and 3 clear grains, respectively, (T2, T3, Table 1, Figure 6A) plot older than those described above and are between the cluster of igneous zircon at 1855 Ma and the dark-brown titanite cluster at 1638 Ma. T3 would fit on a line between these two ages, while T2 falls slightly below the line.

The titanite data imply that there are 3 generations of titanite within the sample of the complex dyke. The simplest interpretation is that there is some relict igneous titanite demonstrated by analysis T2, which is overgrown by a younger metamorphic generation of titanite, or possibly two metamorphic generations at 1638 and *ca.* 1050 Ma. T3 is best explained by relict igneous titanite overgrown by 1638 Ma metamorphic titanite. The dark-brown titanite crystallized at 1638 ± 7.5 Ma, likely at a time of greatest availability of uranium for incorporation into its crystal lattice. Analyses T1 and T4 demonstrate that there was a metamorphic overprint, with some new titanite growth during the Grenvillian Orogeny, but this event is not well established as no analysis is concordant at that time. However, a previously reported sample from the Michelin deposit (GS-08-215; Sparkes and Dunning, 2015), had most of the metamorphic titanite yield Grenvillian ages. It therefore appears that different rocks at different locations within the deposit were

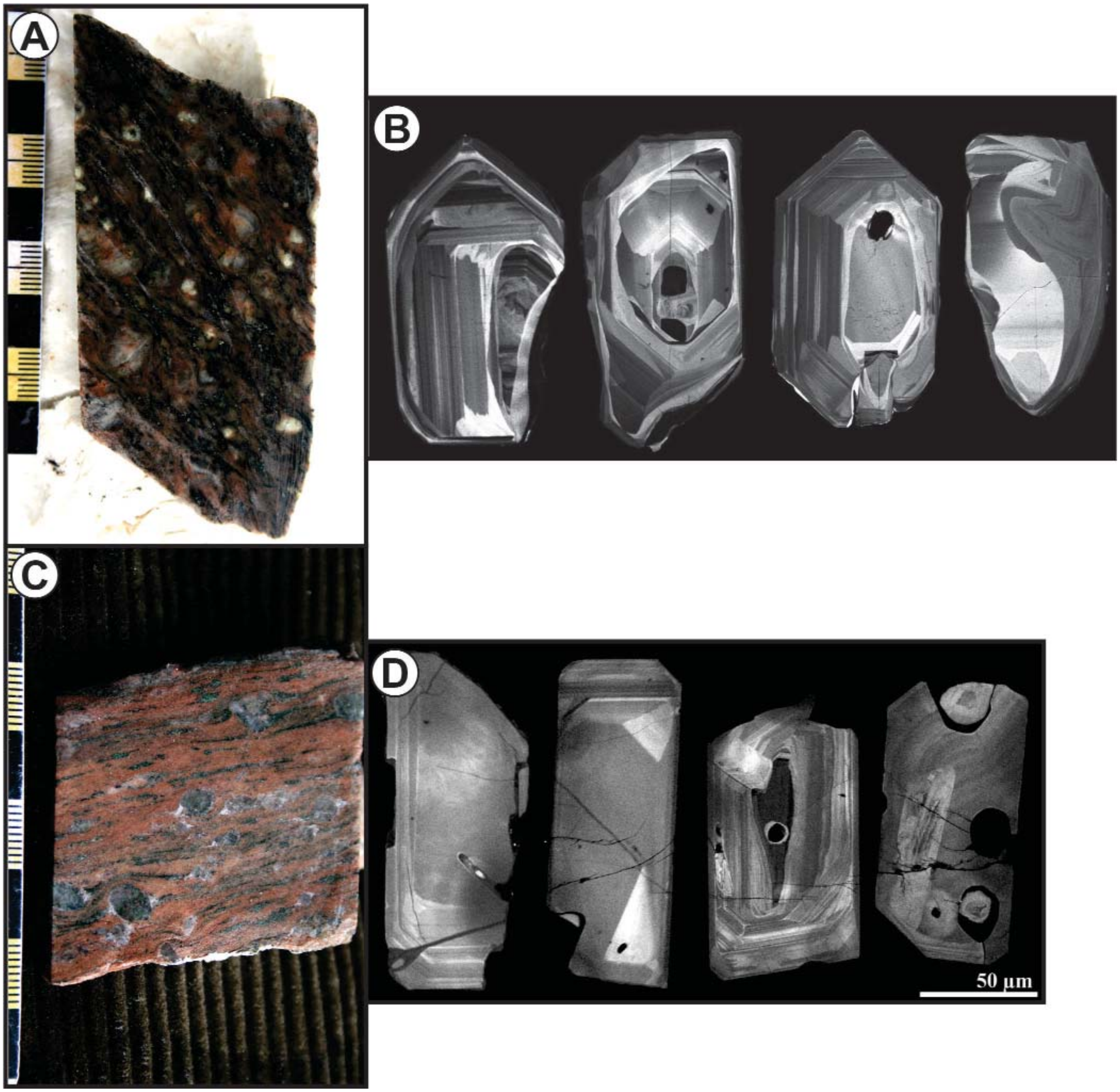

Plate 4. *A) Coarse-grained, quartz- and feldspar-phyric unit, which forms the core of the complex dyke sampled for geochronological study (Sample GS-14-252; DDH ML14-157, 73 m depth); B) Cathodoluminescence images of select zircon from sample GS-14-252, displaying well-developed growth zoning related to igneous crystallization; C) Weakly mineralized quartz–feldspar-phyric, metarhyolite dyke displaying moderate to strong hematite–albite alteration (Sample GS-14-243; DDH ML-163, 375 m depth); D) Cathodoluminescence images of select zircon from sample GS-14-243, displaying growth zoning patterns similar to those developed in sample GS-14-252.*

open to recrystallization and conditions favourable for titanite growth during different metamorphic events. This demonstrates a potential problem with attempting to document all the events affecting a study area from the analysis of only one or a few samples.

A sample of a weakly mineralized coarse-grained, highly quartz- and feldspar-phyric, metarhyolite dyke (coarse porphyritic metarhyolite unit of Evans (1980); coarse-grained porphyritic metamorphosed felsic volcanic unit of Hicks (2015)) was collected to further constrain the age of

Table 1. U–Pb zircon and titanite data for samples discussed in the text; UTM's for each sample are provided in NAD 27, Zone 21 and represent the coordinates for the drillhole collar from which the sample was collected

		Concentration		Measured		Corrected Atomic Ratios*							Age (Ma)		
Fraction	Weight (mg)	U	Pb rad (ppm)	total common Pb (pg)	$^{206}Pb/^{204}Pb$	$^{208}Pb/^{206}Pb$	$^{206}Pb/^{238}U$	±	$^{207}Pb/^{235}U$	±	$^{207}Pb/^{206}Pb$	±	$^{206}Pb/^{238}U$	$^{207}Pb/^{235}U$	$^{207}Pb/^{206}Pb$
GS14-243 – Quartz–Feldspar-phyric Metarhyolite dyke: DDH ML-163; 374.75-375.20 m depth (307249, 6052131)															
Z1 1 clr lrg prm abr	0.001	344	121.9	2.1	3475	0.1247	0.33226	214	5.174	29	0.11294	38	1849	1848	1847
Z2 3 clr prm abr	0.003	54	19.6	4.1	836	0.1507	0.33216	190	5.178	29	0.11306	44	1849	1849	1849
Z3 5 clr euh prm abr	0.005	175	62.6	5.8	3140	0.1416	0.33105	224	5.159	34	0.11302	26	1843	1846	1849
Z4 3 clr lrg prm abr	0.003	270	96.6	3.8	4452	0.1395	0.33199	228	5.172	29	0.11300	46	1848	1848	1848
GS14-252 – Quartz–Feldspar-phyric core of the complex dyke: DDH ML14-157; 72.90-81.06 m depth (307061, 6052200)															
Z1 4 lrg clr euh	0.006	82	30.4	45	242	0.1873	0.32991	114	5.165	25	0.11355	44	1838	1847	1857
Z2 5 lrg clr euh	0.007	196	71.0	1.9	16013	0.1619	0.33003	254	5.156	37	0.11331	32	1839	1845	1853
Z3 1 lrg clr euh	0.002	219	78.3	6.7	1032	0.1515	0.32776	216	5.118	29	0.11325	52	1828	1839	1852
Z4 1 lrg clr euh	0.002	283	102.5	2.6	3375	0.1530	0.33269	186	5.204	22	0.11345	50	1851	1853	1855
T1 1 clr euh	0.002	58	18.5	57	46	0.2081	0.28399	282	3.938	96	0.10058	216	1611	1622	1635
T2 3 clr euh	0.004	192	63.1	14	1247	0.1016	0.31497	172	4.817	25	0.11091	32	1765	1788	1814
T3 1 clr euh	0.002	28	9.1	16	67	0.1501	0.30427	304	4.365	114	0.10404	232	1712	1706	1697
T4 1 clr euh	0.002	54	16.5	9	160	0.3724	0.24000	182	3.046	47	0.09204	126	1387	1419	1468
T5 1 clr dk brn	0.002	207	64.5	20	294	0.1501	0.28912	180	4.011	61	0.10061	132	1637	1636	1635
T6 1 dk brn clr	0.002	507	164.3	61	245	0.1894	0.29190	700	4.032	139	0.10019	256	1651	1641	1628
T7 2 lrg dk brn	0.002	594	202.3	476	63	0.2689	0.28865	364	4.003	107	0.10059	220	1635	1635	1635
T8 1 clr dk brn	0.002	229	76.3	85	91	0.2553	0.28633	320	3.757	140	0.09515	306	1623	1583	1531

Notes: Z=zircon, T=titanite, 1,2=number of grains, lrg=large, clr=clear, dk=dark, brn=brown, prm=prism, euh=euhedral, abr=physically abraded.
All zircon was chemically abraded (Mattinson, 2005). Weights were estimated so U and Pb concentrations are approximate. * Atomic ratios corrected for fractionation, spike, laboratory blank of 1-2 picograms of common lead, and initial common lead at the age of the sample calculated from the model of Stacey and Kramers (1975), and 0.3 picogram U blank. Two sigma uncertainties are reported after the ratios and refer to the final digits.

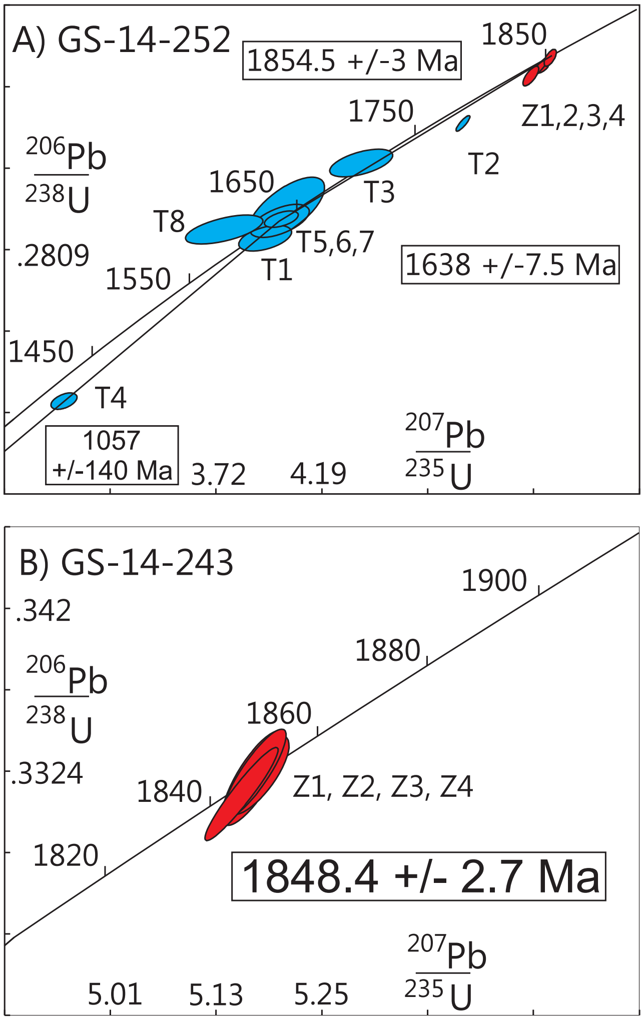

Figure 6. *Concordia diagrams of U–Pb results from zircon (red) and titanite (blue) analyses for samples discussed in the text. Error ellipses are at the 2σ level. Refer to Table 1 for sample location and description.*

mineralization (Sample GS-14-243; DDH ML-163, 375 m depth; Plate 4C). This sample contained 562 ppm U, 462 ppm Zr, 8.17 wt. % Na_2O and yielded both zircon (Plate 4D) and titanite. Initially, this sample was targeted for possible hydrothermal zircon, which has been noted within this and other such deposits (*e.g.*, Hicks, 2015; Cuney *et al.*, 2012). Most large euhedral zircon prisms have thin overgrowths coating them and, locally consist of hydrothermal zircon (Hicks, 2015). However, the rims that were tested as part of this study through SEM analysis all consisted of titanite. All zircon crystals selected for analysis were physically abraded to remove the overgrowths (*cf.* Krogh, 1982), which would have also removed any secondary zircon or titanite of hydrothermal origin, if present. Four analyses of 1 to 5 abraded clear crystals of zircon with low to average U content yield overlapping concordant points (Table 1; Figure 6B) and a weighted average $^{207}Pb/^{206}Pb$ age of 1848.4 ± 2.7 Ma (MSWD = 0.064). This age represents the primary igneous crystallization age of the unit and also provides a new maximum age for the development of uranium mineralization at the deposit. No titanite analyses have yet been carried out for this sample.

SUMMARY AND DISCUSSION

New geochronological data obtained from the highly quartz- and feldspar-phyric metarhyolite dyke, representing the main host to uranium mineralization at the Michelin deposit, indicate the unit represents an unrecognized intrusive event, which is, at least, 4.9 Ma younger then the host crystal tuff. This age provides a new maximum age limit of *ca.* 1851 Ma for the development of uranium mineralization in the area. In addition, dating of the coarse-grained porphyritic felsic core of the complex dyke (1854.5 ± 3 Ma) has produced an age which is unresolvable from that obtained from the host crystal tuff (1858 ± 2 Ma), within analytical error. However, the textural similarities between the felsic core of the complex dyke and the highly quartz- and feldspar-phyric metarhyolite dyke, are suggestive of a common magmatic origin for the two units, representing a period of younger magmatic activity that is separable from the formation of the host volcanic sequence.

Detailed geochemical sampling of outcropping volcanic and plutonic rocks in the area of the Michelin deposit illustrates the distribution of the sodium metasomatism in relation to the development of the albitite-type uranium mineralization, although the latter is poorly developed at surface. Most of the samples displaying sodium-enrichment are located to the east of Michelin and form a northeasterly trend, which is oblique to the main trend defined by the Michelin deposit. Most of the samples displaying sodium-enrichment also displayed variably depleted potassium values, which is characteristic of the sodium metasomatism developed in the area.

The fact that most other known albitite-type uranium mineralization is structurally controlled would imply that a significant regional-scale structure exists within the vicinity of the Michelin deposit. However, recognition of such a structure is hampered by the poor outcrop density in the area. Rarely, well-preserved examples of well-developed brecciation provide supporting evidence for the presence of local brittle deformation in the vicinity of the deposit. As this style of deformation is likely linked with the formation of the albitite-type mineralization, it is inferred to have formed between *ca.* 1851 and 1800 Ma. In addition, the predominance of ductile deformation observed in drillcore, as opposed to the rare occurrences of brecciation, suggests that the latter represents an early event that is subsequently overprinted by later ductile deformation. This later deformation is locally inferred to be as young as Grenvillian in age. Elsewhere in the region, development of uranium mineralization shares a spatial association with steeply dipping shear zones attributed to a regional D_3 event, representing sinistral transpression associated with the westward thrusting of the Aillik Group (Culshaw *et al.*, 2000; Hinchey and LaFlamme, 2009). These structures are locally associated with the development of sodium metasomatism in association with uranium mineralization, such as that developed along the Big Island shear zone (Figure 1).

As indicated by the U–Pb geochronological data obtained from titanite, several periods of metamorphism can be identified within the deposit, with the youngest being Grenvillian in age. The effects of this deformation with respect to the redistribution of the uranium mineralization within the deposit have yet to be fully understood. In addition, the timing of the sodium metasomatism at Michelin, and its potential ties with iron-oxide alkali-altered systems of the western CMB (*cf.* Sparkes *et al.*, 2016) have yet to be fully evaluated and will form the basis of future studies in the region.

REFERENCES

Bailey, D.G.
1979: Geology of the Walker-MacLean Lake area, 13K/9, 13J/12, Central Mineral Belt, Labrador. Government of Newfoundland and Labrador, Department of Mines and Energy, Mineral Development Division, Report 78-3, 17 pages.

Clark, A.M.S.
1979: Proterozoic deformation and igneous intrusions in part of the Makkovik subprovince, Labrador. Precambrian Research, Volume 10, pages 96-114.

Culshaw, N., Ketchum, J. and Barr, S.
2000: Structural evolution of the Makkovik Province, Labrador, Canada: Tectonic processes during 200 Myr at a Paleoproterozoic active margin. Tectonics, Volume 19, No. 5, pages 961-977.

Culshaw, N.G., Ketchum, J.W.F., Barr, S. and Sinclair, G.
1998: A history of the Makkovik Province. In Eastern Canadian Shield Onshore–Offshore Transect (ECSOOT), Report of the 1998 Transect Meeting. Complied by R.J. Wardle and J. Hall. The University of British Columbia, Lithoprobe Secretariat, Lithoprobe Report 68, pages 20-37.

Cuney, M., Emtz, A., Mercadier, J., Mykchaylov, V., Shunko, V. and Yuslenko, A.
2012: Uranium deposits associated with Na-metasomatism from central Ukraine: A review of some of the major deposits and genetic constraints. Ore Geology Reviews, Volume 44, pages 82-106.

Cuney, M. and Kyser, K.
2008: Deposits related to Na-metasomatism and high-grade metamorphism. *In* Recent and Not-so-recent Developments in Uranium Deposits and Implications for Exploration. *Edited by* M. Cuney and K. Kyser. Mineralogical Association of Canada, Short Course Series 39, pages 97-116.

Cunningham-Dunlop, I.R. and Lee, C.
2008: An update on the exploration activities of Aurora Energy Resources Inc. on the CMB uranium property, Labrador, Canada, during the period of January 1, 2007 to December 31, 2007. NI 43-101 F1 Technical Report, 216 pages.

Dahlkamp, F.J.
1993: Uranium Ore Deposits. Berlin, Springer-Verlag, 460 pages.

Davis, D.W.
1982: Optimum linear regression and error estimation applied to U–Pb data. Canadian Journal of Earth Sciences, Volume 19, pages 2141-2149.

Evans, D.
1980: Geology and petrochemistry of the Kitts and Michelin uranium deposits and related prospects, Central Mineral Belt, Labrador. Unpublished Ph.D. thesis, Queen's University, Kingston, Ontario, Canada, 311 pages.

Gandhi, S.S.
1969: Report on the geology of the Kaipokok Bay–Big River area, Labrador. Newfoundland and Labrador Geological Survey, Assessment File 13J/0042, 11 pages.

1970: Report on the surface exploration of the geology of the Michelin prospect in the Kaipokok Bay area, Labrador. Newfoundland and Labrador Geological Survey, Assessment File 13J/0065.

1976: Report on geology, isotopic ages and origin of uranium occurrences in the Kaipokok Bay–Big River area, Labrador. Newfoundland and Labrador Geological Survey, Assessment File LAB/0318, 59 pages.

1978: Geological setting and genetic aspects of uranium occurrences in the Kaipokok Bay–Big River area, Labrador. Economic Geology, Volume 73, pages 1492-1522.

1984: Uranium in early Proterozoic Aillik Group, Labrador. *In* Proterozoic Unconformity and Strata-bound Uranium Deposits. *Edited by* J. Ferguson. IAEA, Vienna, Technical Doc. 315, pages 35-68.

Gower, C.F., Flanagan, M.J., Kerr, A. and Bailey, D.G.
1982: Geology of the Kaipokok Bay–Big River area, Central Mineral Belt, Labrador. Government of Newfoundland and Labrador, Department of Mines and Energy, Mineral Development Division, Report 82-7, 77 pages.

Hertel, M., Podhorski-Thomas, M., Durston, K., Edwards, C. and Allard, S.
2009: Michelin uranium project, Labrador Canada, NI 43-101 technical report on preliminary economic assessment. NI 43-101 F1 Technical Report, 221 pages.

Hicks, C.
2015: Petrological and geochemical investigations of the Michelin uranium deposit, Central Mineral Belt, Labrador. M.Sc. thesis, Memorial University of Newfoundland, St John's, Newfoundland, 464 pages.

Hinchey, A.M.
2007: The Paleoproterozoic metavolcanic, metasedimentary and igneous rocks of the Aillik domain, Makkovik Province, Labrador (NTS map area 13O/03). *In* Current Research. Government of Newfoundland and Labrador, Department of Natural Resources, Geological Survey, Report 07-1, pages 25-44.

Hinchey, A.M. and LaFlamme, C.
2009: The Paleoproterozoic volcano-sedimentary rocks of the Aillik Group and associated plutonic suites of the Aillik domain, Makkovik Province, Labrador (NTS map area 13J/14). *In* Current Research. Government of Newfoundland and Labrador, Department of Natural Resources, Geological Survey, Report 09-1, pages 159-182.

Hinchey, A.M. and Rayner, N.
2008: Timing constraints on the Paleoproterozoic, bimodal metavolcanic rocks of the Aillik Group, Aillik domain, Makkovik Province, Labrador. Geological Association of Canada – Mineralogical Association of Canada, Joint Annual Meeting, Abstract Volume 33.

Kerr, A.
1994: Early Proterozoic magmatic suites of the eastern Central Mineral Belt (Makkovik Province), Labrador: geology, geochemistry and mineral potential. Government of Newfoundland and Labrador, Department of Natural Resources, Geological Survey, Report 94-03, 167 pages.

Kerr, A., Hall, J., Wardle, R.J., Gower, C.F. and Ryan, B.
1997: New reflections on the structure and evolution of the Makkovikian–Ketilidian orogeny in Labrador and southern Greenland. Tectonics, Volume 16, pages 942-965.

Kerr, A., Ryan, B., Gower, C.F. and Wardle, R.J.
1996: The Makkovik Province: extension of the Ketilidian Mobile Belt in mainland North America. *In* Precambrian Crustal Evolution in the North Atlantic Region. *Edited by* T.S. Brewer. Geological Society of London, Special Publication No. 1112, pages 155-177.

Ketchum, J.W.F., Culshaw, N.G. and Barr, S.M.
2002: Anatomy and orogenic history of a Paleoproterozoic accretionary belt: the Makkovik Province, Labrador, Canada. Canadian Journal of Earth Sciences, Volume 39, pages 711-730.

Krogh, T.E.
1982: Improved accuracy of U–Pb zircon ages by the creation of more concordant systems using an air abrasion technique. Geochimica et Cosmochimica Acta, Volume 46, pages 637-649.

Mattinson, J.M.
2005: Zircon U–Pb chemical abrasion (CA-TIMS) method; combined annealing and multi-step partial dissolution analysis for improved precision and accuracy of zircon ages. Chemical Geology, Volume 220, pages 47-66.

Minatidis, D.G.
1976: A comparative study of trace element geochemistry and mineralogy of some uranium deposits of Labrador and evaluation of some uranium exploration techniques in a glacial terrain. M.Sc. thesis, Memorial University of Newfoundland, St. John's, Newfoundland, 239 pages.

Montreuil, J.F., Corriveau, L. and Potter, E.G.
2015: Formation of albite-hosted uranium within IOCG systems: the Southern Breccia, Great Bear magmatic zone, Northwest Territories, Canada. Mineralium Deposita, Volume 50, pages 293-325.

Otto, A., Thomas, W., Barrett, S., Walsh, M. and Jory, J.
2013: The geology of the Michelin Rainbow Trend in the Central Mineral Belt, Labrador. Aurora Energy Internal Report, 30 pages.

Piloski, M.J.
1976: Annual report for 1975 on exploration at the Michelin prospect, Labrador, Part 1. Newfoundland and Labrador Geological Survey, Assessment File 13J/12/0155, 61 pages.

Polito, P.A., Kyser, T.K. and Stanley, C.
2009: The Proterozoic, albitite-hosted, Valhalla uranium deposit, Queensland, Australia: a description of the alteration assemblage associated with uranium mineralization in diamond drill hole V39. Mineralium Deposita, Volume 44, pages 11-40.

Schärer, U., Krogh, T.E., Wardle, R.J., Ryan, B. and Gandhi, S.S.
1988: U–Pb ages of early to middle Proterozoic volcanism and metamorphism in the Makkovik Orogen, Labrador. Canadian Journal of Earth Sciences, Volume 25, pages 1098-1107.

Sharpley, F.J.
1980: Report on the geology and reserves of the Michelin deposit, Labrador. Newfoundland and Labrador Geological Survey, Assessment File LAB/0536, 86 pages.

Sinclair, G.S., Barr, S.M., Culshaw, N.G. and Ketchum, J.W.F.
2002: Geochemistry and age of the Aillik Group and associated plutonic rocks, Makkovik Bay area, Labrador: implications for tectonic development of the Makkovik Province. Canadian Journal of Earth Sciences, Volume 39, pages 731-748.

Sparkes, G.W.
2017a: Uranium mineralization within the Central Mineral Belt of Labrador: a summary of the diverse styles, settings and timing of mineralization. Government of Newfoundland and Labrador, Department of Natural Resources, Geological Survey, Open File LAB/1684, 198 pages.

2017b: Geochemical data from the Central Mineral Belt of Labrador (NTS map areas 13J/09, 10, 12, 13, 14, 15; 13K/02, 03, 05, 06, 07, 09, 10, 11, 14; 13O/03, 04). Newfoundland and Labrador Department of Natural Resources, Geological Survey, Open File LAB/1692, 209 pages.

Sparkes, G.W. and Dunning, G.R.
2009: Preliminary investigations into the style, setting and timing of uranium mineralization, Jacques Lake deposit, Central Mineral Belt, Labrador. *In* Current Research. Government of Newfoundland and Labrador, Department of Natural Resources, Geological Survey, Report 09-1, pages 81-93.

2014: Late Neoproterozoic epithermal alteration and mineralization in the western Avalon zone: a summary of mineralogical investigations and new U–Pb geochronological results. *In* Current Research. Government of Newfoundland and Labrador, Department of Natural Resources, Geological Survey, Report 14-1, pages 99-128.

2015: New U–Pb age constraints on the development of uranium mineralization within the Central Mineral Belt of Labrador. *In* Current Research. Government of Newfoundland and Labrador, Department of Natural Resources, Geological Survey, Report 15-1, pages 105-123.

Sparkes, G.W., Dunning, G.R., Fonkwe, M. and Langille, A.
2016: Age constraints on the formation of iron oxide-rich hydrothermal breccias of the Moran Lake area: Evidence for potential IOCG-style mineralization within the Central Mineral Belt of Labrador. *In* Current Research. Government of Newfoundland and Labrador, Department of Natural Resources, Geological Survey, Report 16-1, pages 71-90.

Sparkes, G.W. and Kerr, A.
2008: Diverse styles of uranium mineralization in the Central Mineral Belt of Labrador: an overview and preliminary discussion. *In* Current Research. Government of Newfoundland and Labrador, Department of Natural Resources, Geological Survey, Report 08-1, pages 193-227.

Stacey, J.S. and Kramers, J.D.
1975: Approximation of terrestrial lead isotope evolution by a two stage model. Earth and Planetary Science Letters, Volume 26, pages 207-221.

Wardle, R.J. and Bailey, D.G.
1981: Early Proterozoic sequences in Labrador. *In* Proterozoic Basins of Canada. Geological Survey of Canada, Paper 81-10, pages 331-359.

Wardle, R.J, Gower, C.F., Ryan, B., Nunn, G.A.G., James, D.T. and Kerr, A.
1997: Geological Map of Labrador; 1:1 million scale.

Government of Newfoundland and Labrador, Department of Mines and Energy, Geological Survey, Map 97-07.

Watson-White, M.V.
1976: A petrological study of acid volcanic rocks in part of the Aillik Series, Labrador. M.Sc. thesis, McGill University, Montreal, Quebec, 132 pages.

Wilde, A.
2013: Towards a model for albitite-type uranium. Minerals, Volume 3, pages 36-48.

Wilde, A., Otto, A., Jory, J., MacRae, C., Pownceby, M., Wilson, N. and Torpy, A.
2013: Geology and mineralogy of uranium deposits from Mount Isa, Australia: Implications for albitite uranium deposit models. Minerals, Volume 3, pages 258-283.

Wilton, D.H.C., McNeil, P., Hicks, C., Tracey, M., Cunningham-Dunlop, I., Lee, C., Thompson, G.M. and Piercey, S.
2010: The nature of uranium mineralization in the Paleoproterozoic Aillik and Post Hill groups, Labrador, Central Mineral Belt. Geological Association of Canada – Mineralogical Association of Canada, Joint Annual Meeting, Abstract Volume, GeoCanada 2010-Working with the Earth.

Wilton, D.H.C. and Wardle, R.J.
1987: Two contrasting granophile and non-granophile metallogenic styles in the Early Proterozoic Upper Aillik Group, Central Mineral Belt, Labrador, Canada. Mineralium Deposita, Volume 22, pages 198-206.